The Effect of Fair-Weather Cumulus Cloud Field Anisotropy on Radiative Surface Fluxes

L. M. Hinkelman and E. E. Clothiaux
Department of Meteorology
Pennsylvania State University
University Park, Pennsylvania

K. F. Evans
Atmospheric and Oceanic Sciences Program
University of Colorado
Boulder, Colorado

T. P. Ackerman
Pacific Northwest National Laboratory
Richland, Washington

Introduction

Recently, substantial efforts have been made to determine the impact of three-dimensional (3D) cloud structure on atmospheric radiative transfer. Unfortunately, 3D high-resolution measurements of cloud field structure are not available for use in these studies. As a result, research in this area has frequently been based on simple stochastic cloud models (e.g., bounded cascades) or extrapolations of two-dimensional (2D) data into three dimensions, both of which assume cloud field isotropy in the horizontal plane. However, the significance of this assumption has not been tested. In this study, a stochastic field generation algorithm (Evans et al. 2001) is used to produce synthetic fair-weather cumulus cloud fields. While the statistics of the output liquid water content (LWC) fields are constrained to match those of sample input fields taken from large-eddy simulations (LES), the vertical and horizontal anisotropy of these fields can be controlled independently. Solar radiative transfer is calculated for a set of fields having a range of anisotropy levels using Monte Carlo methods. The effect of these levels of anisotropy in cloud fields is evaluated by comparing the resulting surface fluxes.

Method

Cloud Structure Measures

Cloud field anisotropy can be broken down into two components. The first is horizontal anisotropy or the degree to which structures in horizontal cross sections of a field have a preferred direction. In this study, horizontal anisotropy is measured using the anisotropy parameter (AP), which is calculated for the power spectrum of the liquid water path (LWP) in half-octave spatial frequency bands according to

$$|A_n| \equiv \frac{\sqrt{M_{c,n}^2 + M_{s,n}^2}}{M_{0,n}}$$

where

$$M_{0,n} = \int_{k_{n-1}}^{k_n} \int_0^{2\pi} S(k,\phi) d\phi dk$$

$$M_{c,n} = \int_{k_{n-1}}^{k_n} \int_0^{2\pi} S(k,\phi) \cos(2\phi)\, d\phi dk$$

$$M_{s,n} = \int_{k_{n-1}}^{k_n} \int_0^{2\pi} S(k,\phi) \sin(2\phi)\, d\phi dk$$

The geometry of the AP calculation is shown in Figure 1. The value of the AP ranges from 0 for isotropic structures to 1 for linear fields. In this work, cloud fields are characterized by the average AP value over the mid- to high-frequency ranges.

Vertical tilt is defined as the horizontal shift in a cloud field per unit height. The displacement between neighboring horizontal LWC cross sections is determined by locating the peak of their 2D cross-correlation function. Tilt for an entire field is specified as the average of these displacements over the entire height of the clouds. Here the cross-correlation functions are found via Fourier methods. Fourier interpolation is used to increase the resolution of peak locations beyond grid spacing.

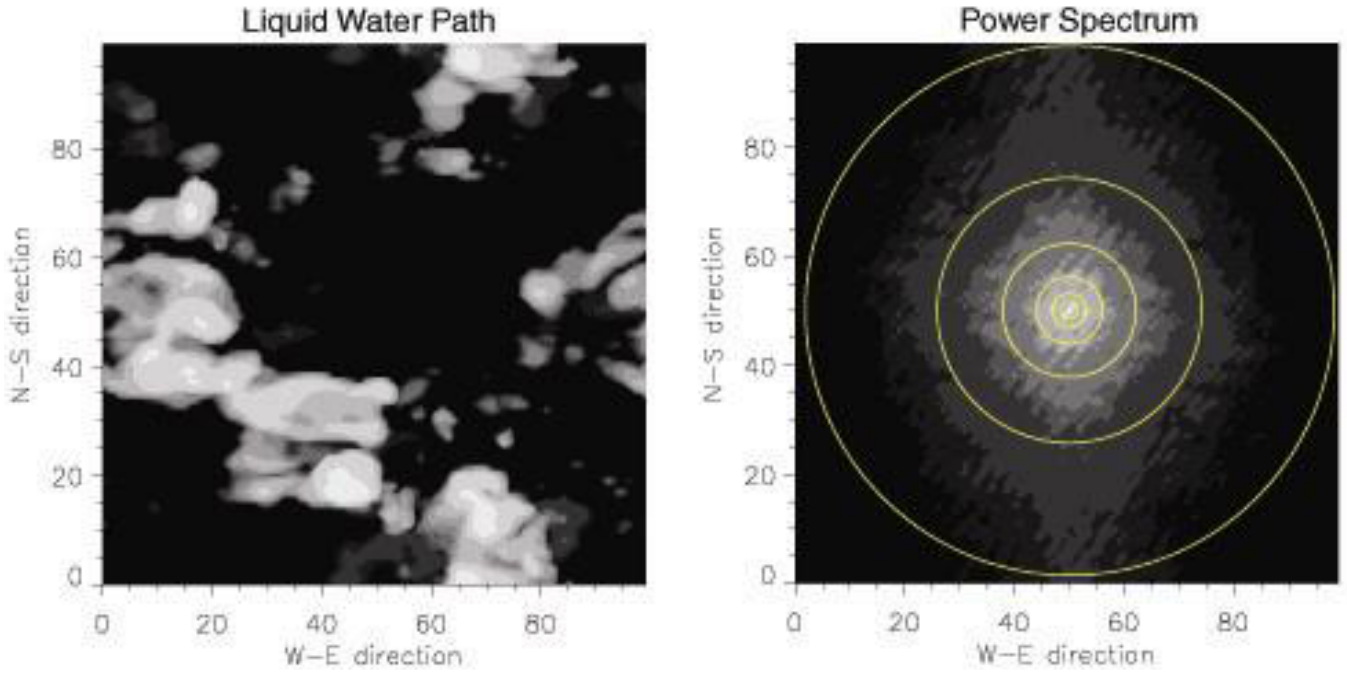

Figure 1. Geometry of AP calculation. Left—sample LWP field. Right—Corresponding power spectrum with octave bands indicated.

Cloud Fields

Synthetic cloud fields are used in this study because their properties can be closely controlled. An individual cloud field can be created and then systematically distorted while maintaining basic characteristics such as the LWC probability density function or total liquid water. The effects of horizontal anisotropy and vertical tilt can thus be separated from other changes in cloud field structure. This is important because the effects of anisotropy are expected to be small.

The stochastic field generator used in this study (Evans et al. 2001) requires various cloud field statistics as input. Here we use statistics calculated for LES output because LES models provide the most realistic high-resolution 3D cloud fields currently available.

We begin with 3D LWC fields produced by the University of California, at Los Angeles (UCLA) LES model (Stevens et al. 1999). The base case simulates continental shallow cumulus forming over the Atmospheric Radiation Measurement (ARM) Southern Great Plains site due to diurnal radiative forcing. The LES grid size is 96 x 96 x 110 with grid spacing of 66.667m x 66.667m x 40.0m. Two scenes from each of six runs with varied initial random potential temperature perturbations provide an ensemble of fields from which to draw statistics. Sample cloud fields used in this study are shown in Figure 2.

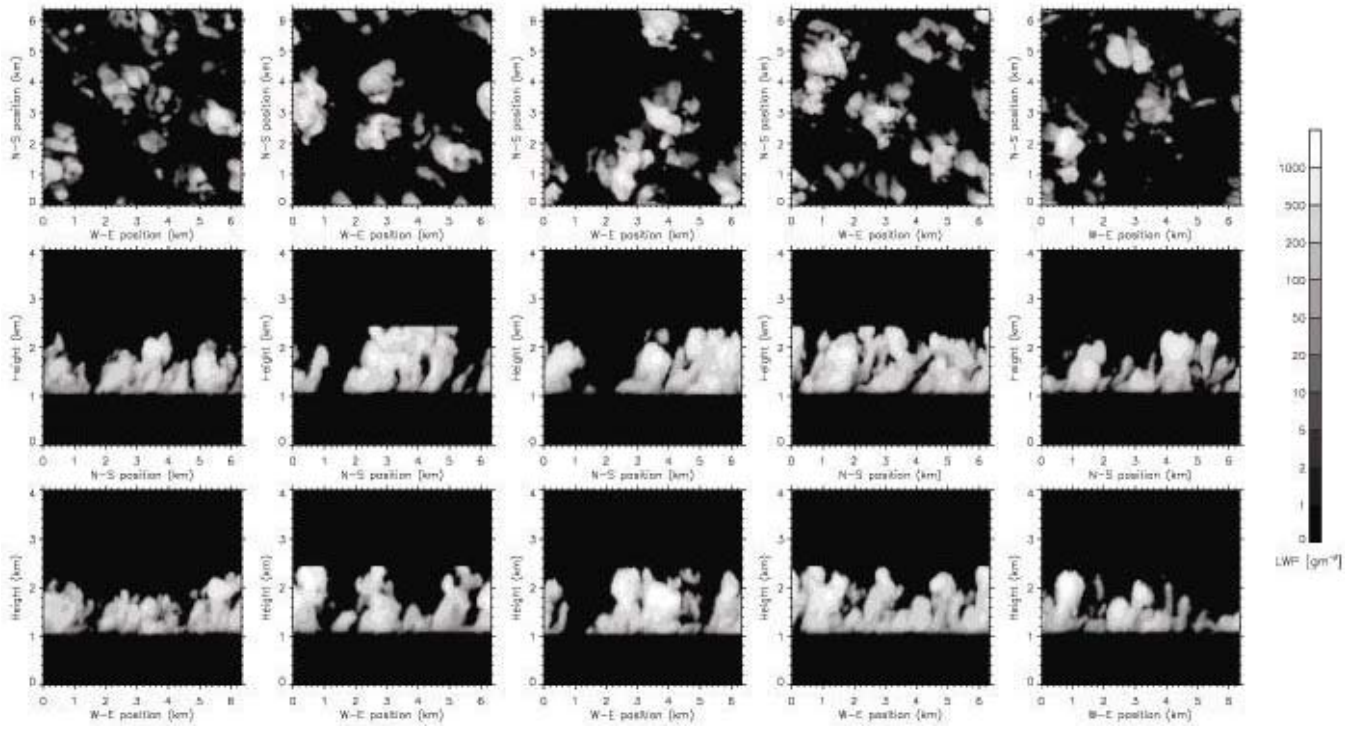

Figure 2. Sample LES cloud fields. For each scene, integrated LWP is shown for views in three directions.

Stochastic cloud field generation follows the method of Evans et al. 2001, with the addition of imposing anisotropy on the fields. Input statistics are the LWC probability density function for each level and the linear correlation functions between cloud masks at each level averaged over a total of 12 LES cloud scenes. The 3D LWC fields of the same size and resolution as the input fields are generated. The basic method of field construction is the filtering of random components in the Fourier domain. Horizontal anisotropy is added by stretching or compressing the axes of the horizontal power spectrum in the Fourier domain such that the clouds are elongated in the horizontal (East/West) direction. Vertical tilt is added by progressively displacing the output LWCs in a scene at each vertical level. Multiple series of cloud fields with a range of tilt and anisotropy levels are produced to allow for statistical analysis of the radiative transfer results. All fields in each series are based on the same random components.

Radiative Transfer Calculations

Domain-average fluxes are calculated for a 0.0175-mm-wide band centered at 0.675 μm using a standard Monte Carlo model tested in ICRCCM-3 (Barker et al. 2002). This model incorporates the Kato band models (Kato et al. 1999). Cloud droplet effective radii are calculated from LWC with cloud drop number density fixed at 300 cm^{-3}. Optical properties for the droplet distributions (single-scattering albedo, asymmetry parameter, and extinction cross section) are calculated using Mie theory. Henyey-Greenstein phase functions are assumed. The surface is considered perfectly absorbing.

Computations are made for solar zenith angles of 0°, 30°, and 60° and azimuthal angles of 0° and 90° azimuthal angles. See Figure 3 for the computational geometry. One million photons are used in each run. Calculations are made for an ensemble of twenty stochastic cloud fields for each solar zenith angle, solar azimuth angle, tilt, and anisotropy combination.

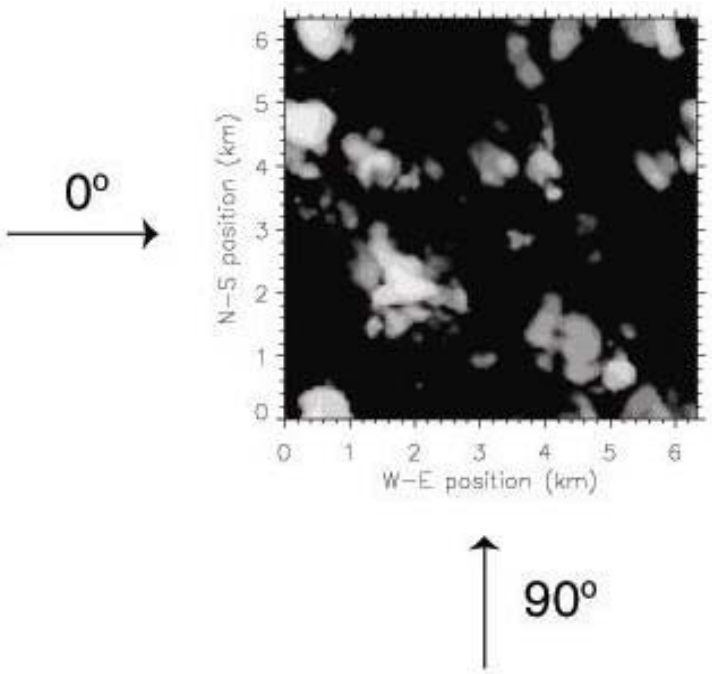

Figure 3. Monte Carlo geometry. Directions of azimuthal angles are shown for a sample cloud field.

Results

A sample sequence of stochastic cloud fields with increasing levels of imposed horizontal anisotropy is shown in Figure 4. The corresponding AP is shown above each field. LES studies indicate that AP values of cloud fields typically range up to about 0.4. Higher APs would occur only in extremely oriented fields, such as when cloud streets are present. Stretching has been imposed in the East-West direction and compression in the North-South direction. Monte Carlo radiative transfer calculations were performed for twenty such sequences.

Transmittance values for the horizontally anisotropic cloud scenes are presented in Figure 5. Increasing anisotropy in the x-direction, increases the cloud cross section presented to solar fluxes traveling perpendicular to the x-axis and thus reduces the solar flux reaching the surface. The opposite is true for fluxes with angles of incidence parallel to the stretching axis. The effects of horizontal anisotropy are more pronounced at large solar zenith angles.

The sequence of tilted clouds made using the same random components as the anisotropic fields of Figure 4 are shown in Figure 6. Note that imposing tilt in the West-East direction leaves the North-South direction unchanged. Tilt is indicated in terms of horizontal displacement per unit vertical rise. The tilts chosen correspond to 0°, 18°, 33°, 45°, and 53° from vertical. Monte Carlo radiative transfer calculations were performed for twenty such sequences.

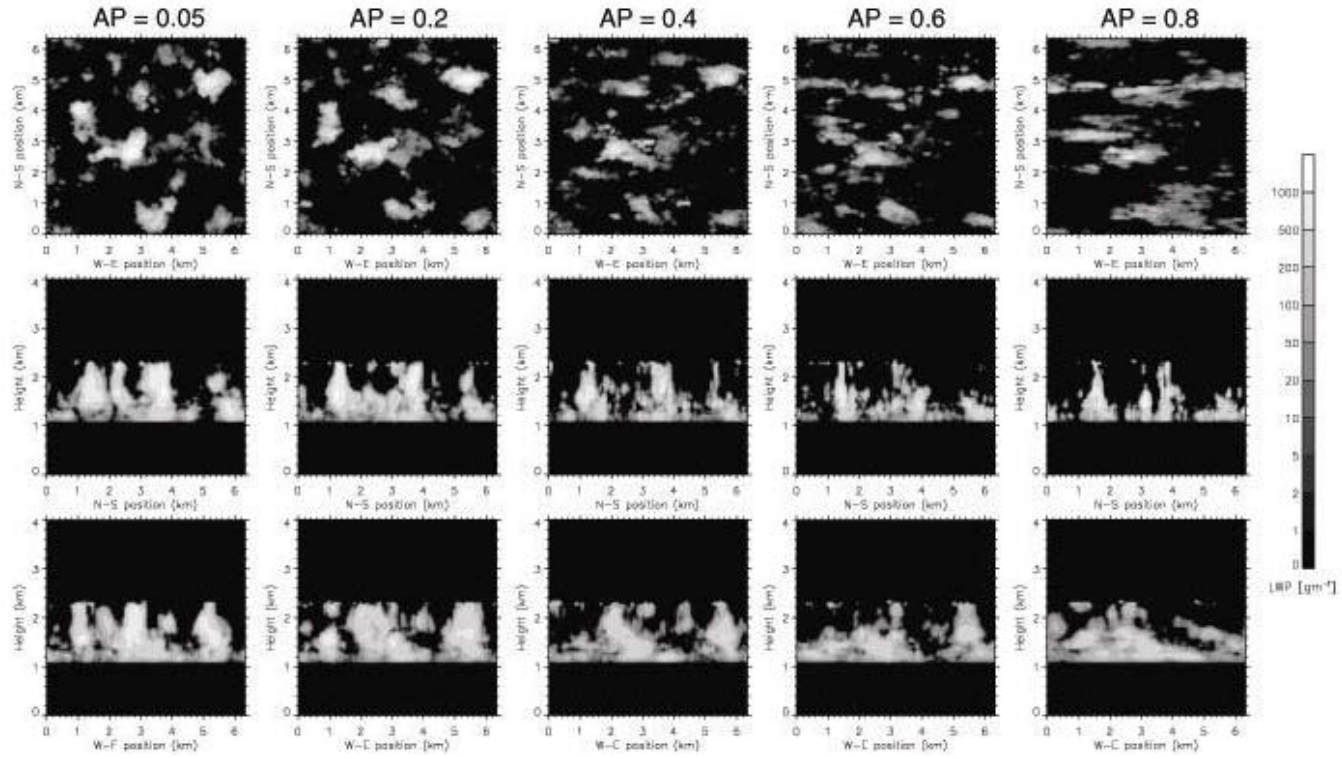

Figure 4. Set of stochastic cloud fields with increasing horizontal anisotropy. For each scene, integrated LWP is shown for views in three directions.

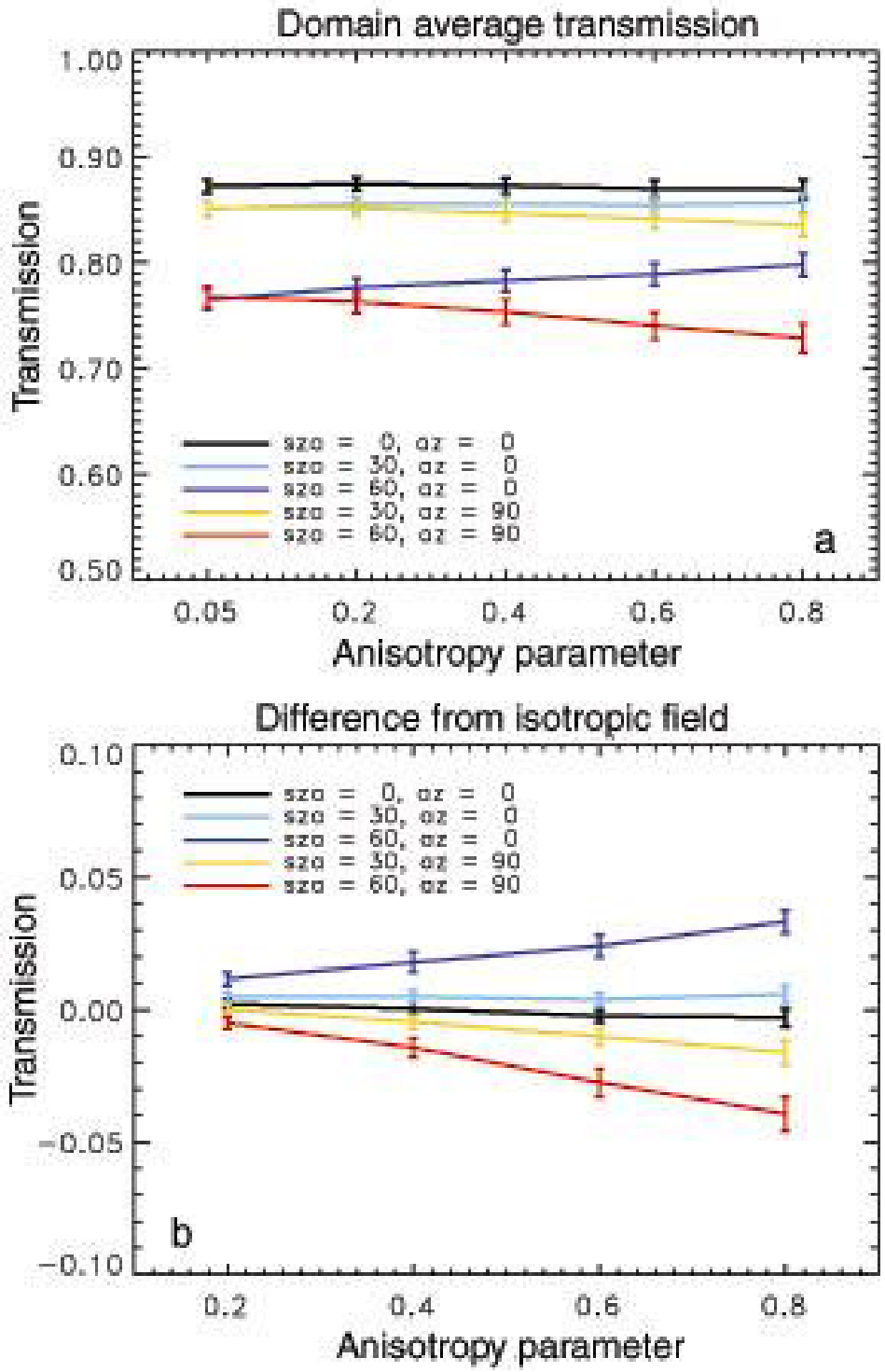

Figure 5. Transmission results for cloud scenes with increasing levels of horizontal anisotropy averaged over all cloud fields for each angle of incidence. (a) Mean total values. (b) Mean differences between results for anisotropic fields and matching isotropic fields. Error bars indicate the standard deviation of the mean.

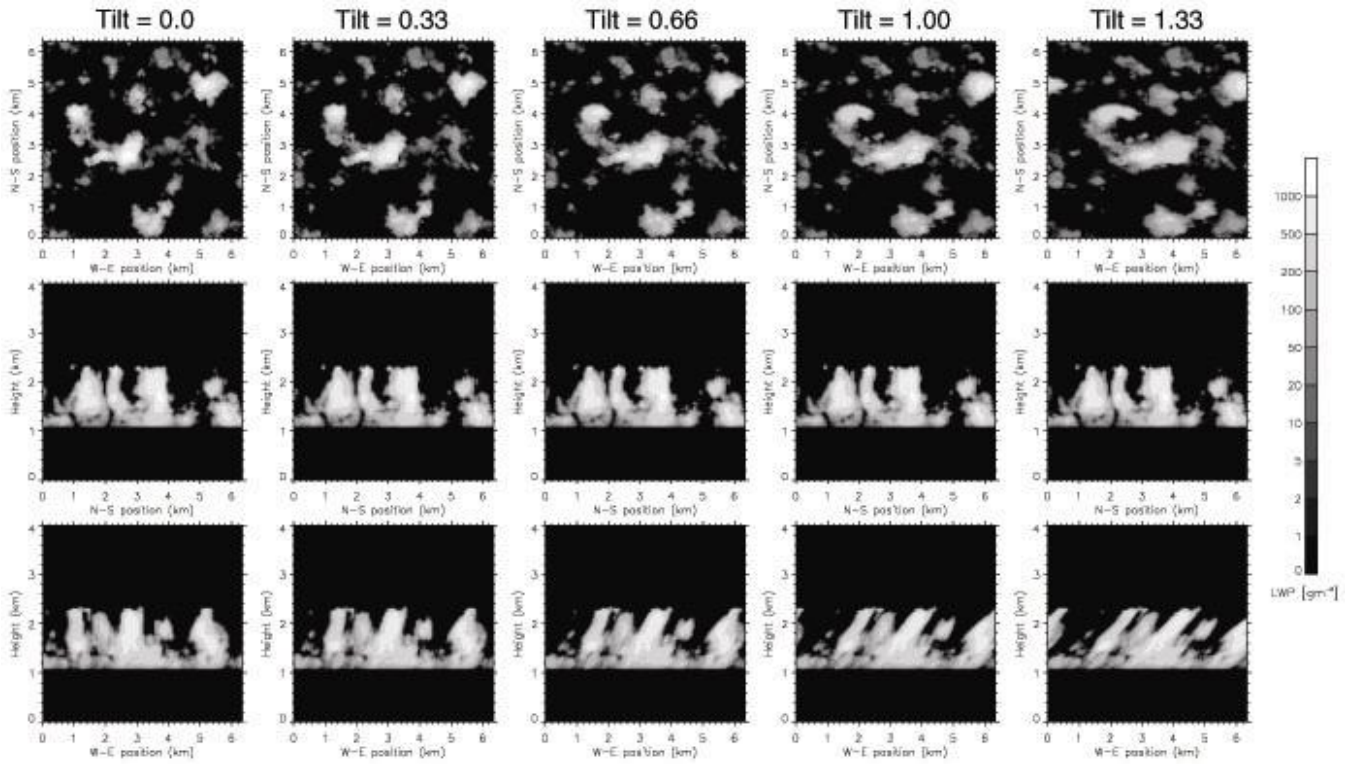

Figure 6. Set of stochastic cloud fields with increasing levels of imposed vertical tilt. For each scene, integrated LWP is shown for views in three directions.

Transmittances calculated for cloud scenes with increasing levels of vertical tilt are shown in Figure 7. Increasing West-East vertical tilt increases the cloud cross section presented to incoming radiation traveling both perpendicular to the x-axis and along the x-axis from the left (up-shear) side. This effect is slight for fluxes impinging on the crosswind sides of the clouds but substantial for fluxes striking the elongated tops of the clouds from the up-shear side. The opposite effect is expected for fluxes incident on the down-shear (right) side of the clouds where tilt will decrease the cloud cross sectional area.

Conclusions

Horizontal anisotropy and vertical tilt of cumulus clouds have a significant effect on domain-average transmitted solar fluxes. To first order, these effects are due to changes in the effective cloud fraction that depend on cloud and radiative geometries.

Future Work

We plan to complete these calculations by including more azimuthal and solar zenith angles, particularly 180° azimuth. Further analysis will be undertaken to determine more precisely what cloud properties of radiative interest (LWP distribution, effective cloud fraction, etc.) change as anisotropy and tilt vary. The study will also be expanded to include broadband solar heating rate profiles as well as domain-averaged broadband transmission and reflection results.

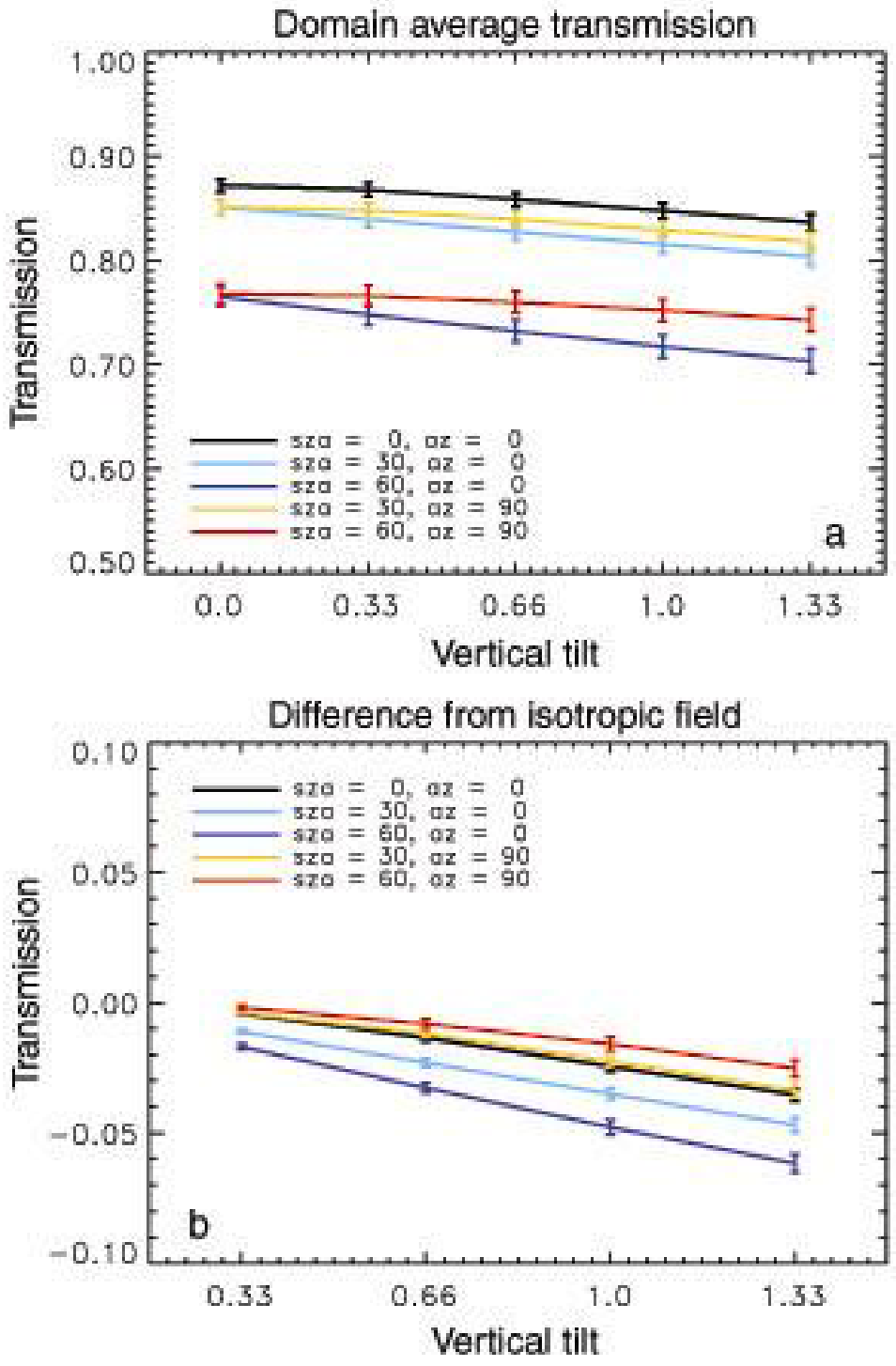

Figure 7. Transmission results for cloud scenes with increasing levels of vertical tilt averaged over all cloud fields for each angle of incidence. (a) Mean total values. (b) Mean differences between results for tilted fields and matching untitled fields. Error bars indicate the standard deviation of the mean.

Corresponding Author

L. M. Hinkelman, laura@essc.psu.edu, (814) 863-5375

References

Barker, H. W., et al., 2002: Assessing 1D atmospheric solar radiative transfer models: Interpretation and handling of unresolved clouds. *J. Climate*, submitted.

Evans, K. F., S. A. McFarlane, and W. J. Wiscombe, 2001: The importance of three-dimensional radiative transfer in small cumulus cloud fields derived from the NAURU MMCR and MWR. In *Proceedings of the Eleventh Atmospheric Radiation Measurement (ARM) Science Team Meeting.* Available URL: http://www.arm.gov/docs/documents/technical/conf_0103/evans-kf.pdf

Kato, S., T. P. Ackerman, J. H. Mather, and E. E. Clothiaux, 1999: The k-distribution method and correlated-k approximation for a shortwave radiative transfer model. *J. Quant. Spectrosc. Radiat. Transfer*, **62**:109-121.

Stevens, B., C.-H. Moeng, and P. P. Sullivan, 1999: Large-eddy simulations of radiatively driven convection: Sensitivities to the representation of small scales. *J. Atmos. Sci*., **56**(23):3963-3984.